JACS
JOURNAL OF THE AMERICAN CHEMICAL SOCIETY

Article

pubs.acs.org/JACS

Rational Design of Polynuclear Organometallic Assemblies from a Simple Heteromultifunctional Ligand

Long Zhang, Yue-Jian Lin, Zhen-Hua Li, and Guo-Xin Jin*

State Key Laboratory of Molecular Engineering of Polymers, Collaborative Innovation Center of Chemistry for Energy Materials, Department of Chemistry, Fudan University, Shanghai 200433, PR China

Supporting Information

ABSTRACT: In modern coordination chemistry, supramolecular coordination complexes take advantage of ligand design to control the shapes and sizes of such architectures. Here we describe how to utilize starting building blocks and a multifunctional ligand to rationally design and synthesize different types of discrete assemblies. Using a hydroxamate ligand featuring two pair of chelating sites together with half-sandwich iridium and rhodium fragments, we were able to construct a series multinuclear organometallic macrocycles and cages through stepwise coordination-driven self-assembly. Experimental observations, supported by computational work, show that selective coordination modes were ascribed to the significant electronic density differences of the two chelating sites, (*O*,*O*′) and (*N*,*N*′). The results underline the advantages of the discrimination between soft and hard binding sites, and suggest that hydroxamic acids can be used as a versatile class of facile multifunctional scaffold for the construction of novel two-dimensional and three-dimensional architectures.

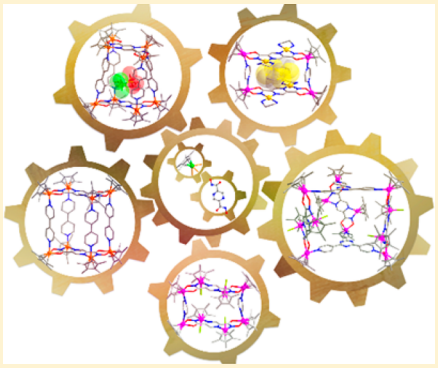

INTRODUCTION

Over the past decade, considerable progress has been made in the chemistry of supramolecular coordination complexes (SCCs).[1−3] A large number of discrete two-dimensional (2D) metallacycles and 3D metallacages displaying intriguing structures with well-defined shape- and size-tunability[4] and promising applications[5] have been prepared by design, using metal−ligand bonds. To achieve predictable architectures, the self-assembly process has to be optimized by taking into account inherent preferences for particular coordination geometries and binding motifs, which are "encoded" in certain molecules depending on the metals and functional groups present.[6] Thus, it is vital to make a judicious choice of metal-containing subunits and organic ligands with multifunctional groups.

Often, multidentate ligands are used to create architectures of increasing scale and complexity, but it is difficult to design and control the shapes and sizes of target structures.[7] This is especially true if selective coordination are required. According to the hard and soft acids and bases theory (HSAB), one promising method is to explore a ligand with two or more binding sites, which have significantly electronic density differences.[8] Hydroxamic acids, a very important family of chelating bioligands, have been widely investigated in both coordination chemistry and chemical biology.[9] However, only a few examples of these hydroxamic acid ligands have been used as building blocks to construct 2D metallacycles or 3D metallacages.[10] This is surprising considering that such ligands are easily accessible, and especially α-aminohydroxamic acids[11] can function as a rigid bridging ligand with two different types of chelating sites, (*O*,*O*′) and (*N*,*N*′).

In recent years, organometallic half-sandwich fragments Cp*M (M = Ir, Rh; Cp* = η^5-*penta*methyl-cyclopentadienyl) and (*p*-cymene)Ru have proven to be versatile metal-containing subunits for the construction of supramolecular organometallic frameworks.[12] Such polynuclear organometallic assemblies have been discussed for their various potential applications, including host−guest chemistry,[13] catalysis,[14] sensors[15] and drug delivery.[16] Given this potentially useful characteristic, we embarked on detailed synthetic and structural studies into the formation of 2D metallacycles and 3D metallacages bearing Cp*M subunits and a new multifunctional ligand pyrazine-2,5-dihydroxamic acid (H_2LK_2). Here, we reported the construction of different types of 2D and 3D discrete supramolecular architectures, facilitated by differences in the electron-donating ability of the two chelating sites. It was confirmed from experimental and theoretical results that the ligand *L* appeared to be a promising scaffold for construct novel SCCs by taking advantage of the discrimination between soft and hard binding sites.

RESULTS AND DISCUSSION

The ligand H_2LK_2 was prepared through the reaction of pyrazine-2,5-dicarboxylic acid dimethyl ester with hydroxylamine. The hydroxamic acid H_2LK_2 can exhibit several tautomeric and resonance structures: **A**, **B** (hydroxamate

Received: August 20, 2015
Published: October 6, 2015

DOI: 10.1021/jacs.5b08826
J. Am. Chem. Soc. 2015, 137, 13670−13678

anion) and **C**, **D** (hydroximate dianion) (Scheme 1). It also displays two types of bidentate chelating sites: the "soft" *N,N′* site, and the electronegative and "hard" *O,O′* site.

Scheme 1. Structures of H2*L* and *L*

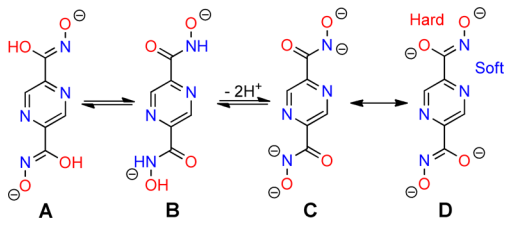

Homometallic Complexes. After treatment with AgOTf (8.0 equiv), solutions of $[Cp^*MCl_2]_2$ (M = Ir, Rh) (2.0 equiv) in methanol were added to a mixture of H_2LK_2 (1.0 equiv) with a few milliliters of DMF in methanol (Scheme 2). Deep green solutions formed, which upon treatment with diethyl ether led to the precipitation of **1a** or **1b**. It is interesting to note that a significant change of color was observed from dark red to deep green after dropping several drops of coordinating solvent (such as CH_3OH and CH_3CN) into a solution of **1a** in CH_2Cl_2. A similar color change was also found if the dried dark red powders of **1a,b** were placed in a moist environment. The dark red color is a feature of unsaturated $16e^-$ derivatives.[17] This significant color change is caused by the change in geometry of the half-sandwich metal centers, from unsaturated five-coordinate to six-coordinate by the binding of coordinating solvent, which may be expected to raise the energies of the metal−ligand antibonding orbitals.[17a] The structures of **1a,b** were confirmed by ^1H NMR spectroscopy and single-crystal X-ray diffraction (Figure S2).

Suitable crystals of **1a** were obtained from slow diffusion of hexane into a solution of **1a** in CH_2Cl_2 and crystals of **1b** were grown by slow diffusion of diethyl ether into CH_3OH. In the structure of **1a**·$2H_2O$, the coordination geometry around the two *O,O′*-bonded iridium atoms is best described as a two-legged piano stool. This 16-electron structure is presumably stabilized by π donation from two oxygen atoms to the metal center.[18] The other two *N,N′*-bonded iridium centers are coordinated by two water molecules, forming a three-legged piano stool geometry. However, crystals of **1a** obtained from vapor diffusion of diethyl ether into an acetonitrile solution of **1a** show a structure in which acetonitrile coordinates to the iridium atoms, generating a saturated six-coordinate complex (Figure S3). The structure of **1b**·$4CH_3OH$ is similar to **1a**·$4CH_3CN$, all rhodium atoms adopt 18-electron configuration due to the binding of methanol. The length of the C(3)−N(2) bond (1.285(13) Å) and C(3)−O(1) bond (1.322(12) Å) in the crystal structure of **1a**·$2H_2O$ reflects considerable C═N double bond and C−O single bond character, respectively. In the 18/18-electron species **1a**·$4CH_3CN$, however, an increase in the C(3)−N(2) (1.316(11) Å) bond length is coupled to a decrease in the C(3)−O(1) (1.295(10) Å) bond length. Taken together, the bond length data from these tetranuclear complexes (Table S3) suggest that the dominant resonance structure of *L* in the 16/18-electron complexes is **D**, while that in the 18/18-electron complexes is **C**.

Octanuclear cages were constructed by using $[(Cp^*M)_4L]^{4+}$ (**1a,b**) as building blocks, which can subsequently be connected by bidentate bridging ligands. Depending on the orientation of the ligands, the octanuclear cages can adopt approximate D_2 or C_{2h} point symmetries where the metal ions define the vertices of a cuboid. Pyrazine was initially used as the bridging ligand, from which reaction we obtained the crystal structure of **2b**-C_{2h} (Figure S5). However, the ^1H NMR spectra of **2a** and **2b** are

Scheme 2. Synthesis of Homometallic Complexes

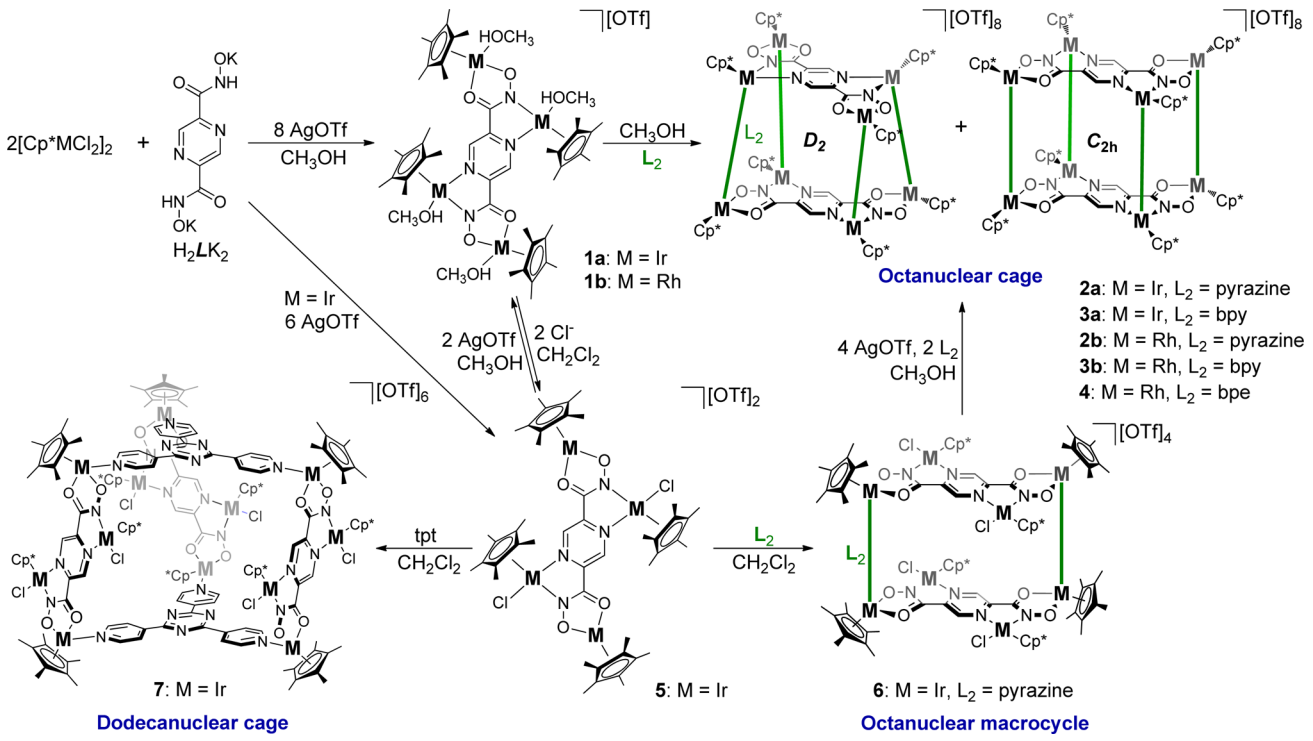

DOI: 10.1021/jacs.5b08826
J. Am. Chem. Soc. 2015, 137, 13670−13678

complicated and cannot be assigned. As no evidence could be gathered for the formation of the D_2 isomer, we decided to use 4,4′-bipyridine (bpy) as the bridging ligand. Two sets of opaque crystals with different crystalline aspects were isolated by vapor diffusion of diethyl ether into a methanol solution of **3b**. The resulting single-crystal X-ray analyses (Figure 1a,b) revealed that two diastereoisomers have crystallized separately.

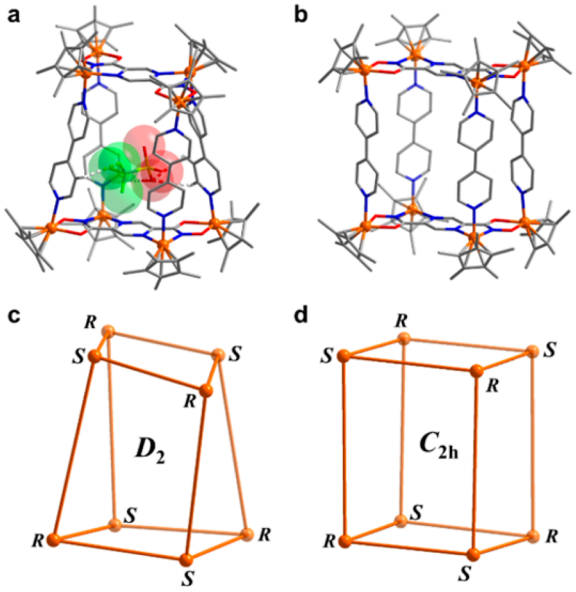

Figure 1. X-ray crystal structure of cationic parts of octanuclear cage $OTf^- \subset$ **3b**-D_2 and **3b**-C_{2h}. (a) Side view of $OTf^- \subset$ **3b**-D_2. (b) Side view of **3b**-C_{2h}. (c) Side view of the D_2 structure with the stereochemical configuration of metal centers labeled. (d) Side view of the C_{2h} structure with the stereochemical configuration (R/S) of metal centers labeled. External anions and hydrogen atoms are omitted for clarity except for involved in hydrogen bonding (N, blue; O, red; C, gray; F, green; S, yellow; Rh, orange).

In both isomers, two $[(Cp^*Rh)_4L]^{4+}$ building blocks are bridged by four bpy ligands to create cage-like complexes with approximate D_2 and C_{2h} point symmetries. In **3b**-D_2, the $[(Cp^*Rh)_4L]^{4+}$ fragment is twisted by 60° with respect to the other; the *O*,*O*′-bonded rhodium centers thus sit directly opposite the *N*,*N*′-bonded rhodium centers. Each metal center of *R* configuration is linked to three other *S* metal centers, with the inverse being true of the *S* metal centers (Figure 1c). The four bpy ligands of **3b**-D_2 slightly bend to adjust to the length difference of adjacent rhodium centers (4.88 Å in one direction and 7.90 Å in the other). Notably, there is a triflate anion hosted in the cavity, stabilized by weak hydrogen bonding to the bpy protons, with the C−H···O−S and C−H···F−C distances in the range 2.67−2.74 Å. The single crystal structure of $OTf^- \subset$ **3a**-D_2 (Figure S6) is almost the same as $OTf^- \subset$ **3b**-D_2, except with iridium centers in place of rhodium centers. The structure of **3b**-C_{2h} is a right parallelepiped-shaped cage with eight Cp*Rh fragments as the corners (Figure 1b,d). The two tetranuclear building blocks lie parallel to each other and are linked by the axial ligands. However, no triflate anion was found in the cavity of this cage.

The solution structure also supports the solid-state structure. The ^{1}H NMR spectrum of $OTf^- \subset$ **3b**-D_2 (Figure S25) gave exclusively peaks corresponding to the D_2-symmetric diastereomer. For the mixture of **3a**,**b**, there are some minor peaks in the ^{1}H NMR spectra presumably corresponding to other minor isomers, but two distinct sets of NMR peaks suggest that most of the samples upon self-assembly exist as two diasteromers. A ^{1}H diffusion-ordered spectroscopy (DOSY) NMR spectrum of **3a** (Figure S22, CD_3OD-d_4) showed that the signals for the aromatic and Cp* units displayed similar diffusion constants, confirming the presence of two diastereoisomers. Furthermore, the appearance of a new signal in the ^{19}F NMR spectra of **3a**,**b** confirmed the encapsulation of an OTf^- anion. In the ^{1}H NMR spectrum of **3a**, **3a**-D_2 and **3a**-C_{2h} were observed in a 4:1 ratio. However, according to the ^{19}F NMR, the host−guest: empty-cage ratio was about 8:5. We inferred that there exists a certain amount of an empty D_2 isomer, which means a template was not required for the formation of D_2 isomer. Gratifyingly, a crystal structure of the empty **3b**-D_2 cage (Figure S7) was obtained, further supporting the suggestion that the construction of the D_2 isomer is not through an anion-templated process.

The isomerization may be thermodynamically driven, as there are more D_2 isomers in the mixture. The ^{1}H NMR spectrum (Figure S27) showed that the reaction temperature can affect the population of the two diasteromers in solution. When the reaction was carried out in methanol at 300 K, the D_2:C_{2h} ratio is about 8:5, while at 338 K the ratio is about 5:1. Once the assemblies had formed, no conversions were observed after heating a sample of either pure $OTf^- \subset$ **3b**-D_2 or the mixture of **3b** at 323 K for 1 week, indicating that the skeleton structure of both isomers is relatively stable in solution state.

To further investigate the isomerization, we tested a longer bridging ligand bpe (trans-1,2-bis(4-pyridyl) ethylene). Both isomers were also observed in this system, as evidenced by ^{1}H NMR spectra (Figure S28). The two isomers in solution were observed in a 8:1 ratio, suggesting that the longer ligand also favored the D_2 isomer. However, the ^{19}F NMR spectrum of **4** showed only one sharp peak, which suggests that it is more energetically favorable for the larger cage to remain empty than for it to adapt to bind the OTf^- anion. The crystal structure of **4**-D_2 (Figure S8) confirmed the absence of the OTf^- anion within the capsule.

Taking advantage of the thermal stability of the 16-electron *O*,*O*′-bonded metal centers, we speculated that the *N*,*N*′-bonded metal centers of the tetranuclear building block $[(Cp^*M)_4L]^{4+}$ would be more favorable toward the generation of 18-electron chloride adducts. Then, open cages could be prepared if the tetranuclear building blocks were connected by bridging ligands through the remaining two vacant sites of the coordinative unsaturated *O*,*O*′-chelated Ir cores (Scheme 2).

After treatment with AgOTf (6.0 equiv), $[Cp^*IrCl_2]_2$ (2.0 equiv) reacted with H_2LK_2 (1.0 equiv) at room temperature, affording tetranuclear complex **5**, as confirmed by ^{1}H NMR spectroscopy. The X-ray structure of **5** (Figure 2a) confirmed the exact coordination modes of the iridium centers. As expected, the *O*,*O*′-bonded iridium centers display an unsaturated five-coordinate structure and the *N*,*N*′-bonded iridium centers have 18-electron configurations due to the binding of chloride ligands.

However, attempts to synthesize analogous Cp*Rh complexes failed to produce pure products, which indicated the great influence of the metal source. To understand why replacing Ir with Rh will not give **5**, charge population analyses and density functional theory (DFT) binding energy calculations were performed (see Supporting Information). It can be seen that the negative charges of the *L* ligand are mostly

DOI: 10.1021/jacs.5b08826
J. Am. Chem. Soc. 2015, 137, 13670−13678

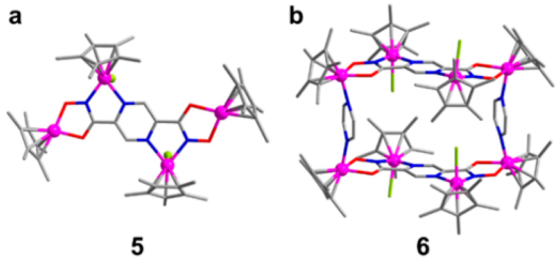

Figure 2. Cationic part of the crystal structure of (a) **5** and (b) **6**. Hydrogen atoms, OTf^- anions, solvent molecules and disorder are omitted for clarity (N, blue; O, red; C, gray; Cl, lime; Ir, pink).

located on the oxygen atoms (−0.92e and −0.82e) (Figure S1). Therefore, after binding with the oxygen atoms it is energetically less favorable for the metal ions to bind to the chloride anion. This can be verified from the binding energies (Table S1). The binding energy of Cl^- with the metal centers bound to the nitrogen atoms are higher than with those bound to the oxygen atoms. It can also be concluded that the bonding of Cl^- to Ir in **5** is stronger than to Rh. In addition, the binding of Cl^- in **5** is more selective if the metal atom is Ir since the binding energy of Cl^- to nitrogen-bound Ir centers is higher than that to the oxygen-bound Ir centers by 30.7 kcal/mol while for Rh this energy difference is just 26.7 kcal/mol.

Similarly, the tetranuclear building block **5** can react with bridging ligands pyrazine and tpt (2,4,6-tri(4-pyridyl)-1,3,5-triazine), affording octanuclear metallamacrocyle **6** and dodecanuclear metallocage **7**, respectively (Figure 3a). In

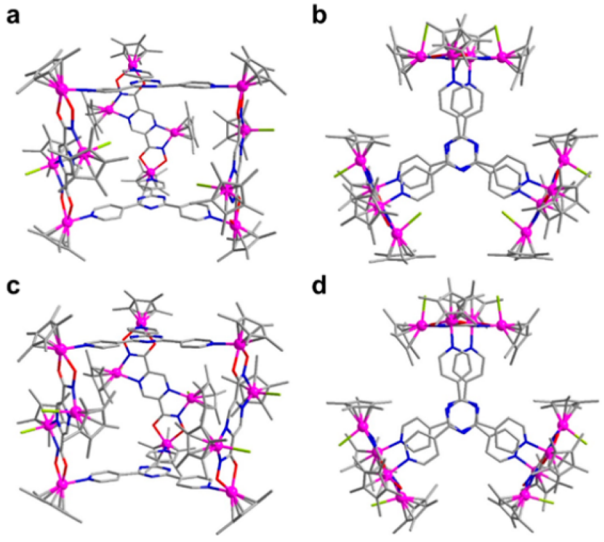

Figure 3. Cationic part of the crystal structure of *S*-**7**. (a,b) Side and top view of *S*-**7**(i). (c,d) Side and top view of *S*-**7**(ii). Hydrogen atoms, OTf^- anions, solvent molecules and disorder are omitted for clarity (N, blue; O, red; C, gray; Cl, lime; Ir, pink).

addition, when 4.0 equiv of AgOTf and 2.0 equiv of pyrazine was added to a CH_3OH solution of the open octanuclear macrocycle **6**, the octanuclear cage **2a** formed. The ^1H DOSY NMR spectra of both **6** and **7** (Figure S34, S36) showed that the aromatic and Cp* signals displayed a single diffusion constant, suggesting that only one stoichiometry of assembly was formed in each case.

The crystal structure of **6** revealed the complex cation to be a half-sandwich iridium metallamacrocycle, which adopts a centrosymmetric structure (Figure 2b). The four *O*,*O*′-bonded Ir atoms that are connected by the bridging pyrazine ligands participate in the 24-membered macrocycle, while the other four *N*,*N*′-bonded Ir atoms, which are coordinated by chloride ligands, can be seen as accessories of the macrocycle.

Single crystals of **7** were grown by slow diffusion of hexane into a solution of **7** in CH_2Cl_2. X-ray diffraction of **7** confirmed the dodecanuclear structure, and showed that complex **7** is a racemic mixture. In the solid state, complex **7** could display different diastereomers due to the orientation of the Cl ligands, facing either "in" or "out" of the cage. Only two of them are found in this assembly: (i) two neighboring Cl ligands on different tetranuclear building blocks are oriented toward the center of the cage (Figure 3a,b); (ii) all six Cl ligands are on the outside of the structure (Figure 3c,d). In case (ii), all Cp* groups are oriented toward the center of the cage, and as a result, the distance between the central triazine rings (10.8 Å) is slightly longer than that of case (i) (10.4 Å) due to steric hindrance. Within each isomer, every Ir center at the corner of the trigonal prism structure has the same coordination stereochemistry (*R* or *S*). The combination of these different chiralities leads to the two *S*-**7** isomers (Figure 3) plus their enantiomers *R*-**7** (Figure S9).

Heterometallic Complexes. To increase the size of the cavity of the self-assembled structures and to create more complexity, we considered heterometallic systems. Based on HSAB theory, we inferred that ***L*** could be a suitable ligand for taking advantage of the differing hardness of the *O*,*O*′ (hard) and *N*,*N*′ (soft) chelating sites, which may lead to selective coordination with different metal centers. While in most instances the hydroxamates can form stable metal complexes through the two oxygen atoms of the hydroxamate functional group with hard transition metals,[9a,c] complexes of hydroxamate ligands with the softer platinum-group metals in other coordination modes have also been reported.[19] Thus, $[Pd(en)]^{2+}$ (en is ethane-1,2-diamine) was selected as the second metal ion, and the relatively soft nitrogen donors of the en group would prevent the possible formation of complex polymeric species.

The heterometallic complexes **9a,b** were isolated as the products of self-sorting reactions (Scheme 3). Upon addition of

Scheme 3. Synthesis of Heterometallic Complexes

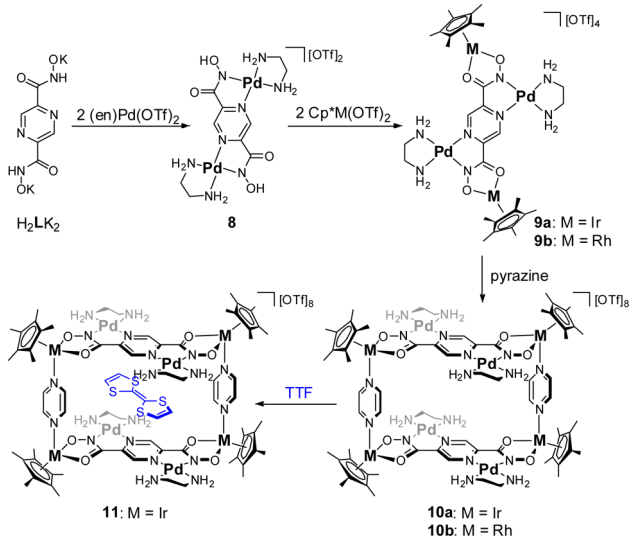

DOI: 10.1021/jacs.5b08826
J. Am. Chem. Soc. 2015, 137, 13670−13678

2.0 equiv of $Cp^*M(OTf)_2$ (M = Ir, Rh) to a purple-red solution of **8** (1.0 equiv) in a mixture of MeOH/DMF, a rapid color change to a dark green solution was observed. As a result of the self-sorting reaction, **9a**,**b** were isolated as dark green crystals. The structure of heterometallic complex **9b** was established by X-ray crystallography (Figure 4), in which Rh ions bind the

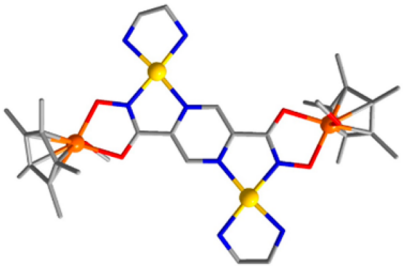

Figure 4. Cationic part of the crystal structure of **9b**. Hydrogen atoms, OTf^- anions, solvent molecules and disorder are omitted for clarity (N, blue; O, red; C, gray; Rh, orange; Pd, gold).

(*O*,*O*′) sites and Pd ions the (*N*,*N*′) sites. The theoretical calculations (Table S2) also support the selective binding of metal ions since the potential energies of **9** are lower than that of **9**′ (by exchanging Ir/Rh and Pd in **9**) by 12.4 and 17.6 kcal/mol, respectively.

Reaction of **9a**,**b** (1.0 equiv) with pyrazine (1.0 equiv) afforded the heterometallic macrocycles **10a**,**b** (Scheme 3). Isomers are not observed in this case. The structures of **10a**,**b** were confirmed by single-crystal X-ray diffraction analysis. The cation of **10a** was found to be a heterometallic macrocycle composed of two heterometallic tetranuclear building blocks (**9a**) which are connected by two pyrazine ligands, with dimensions of 11.12 and 6.94 Å (Ir···Ir nonbonding distances, Figure 5a). The overall structure of the tetranuclear part of the macrocycle is close to planar with slight bends toward the en ligands. Similar to that of **6**, two pyrazine ligands apparently curve inward, with a distance of 9.62 Å between the two pyrazine planes. Two OTf^- anions were found between two neighboring macrocycles, linked by the hydrogen bonds formed

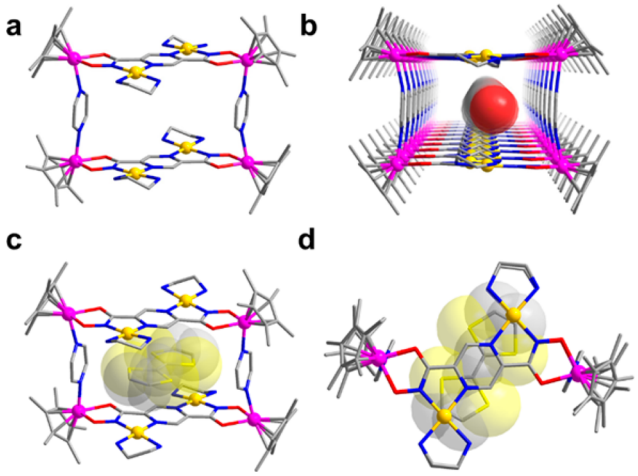

Figure 5. X-ray crystal structure of cationic parts of heterometallic cage **10a** and **11**. (a) Side view of **10a**. (b) Stacking of the molecules in crystals of **10a** viewed along the *z* axis. (c,d) Side and top view of **11**. Hydrogen atoms and OTf^- anions are omitted for clarity (N, blue; O, red; C, gray; S, yellow; Ir, pink; Pd, gold).

between the NH_2/CH_2 protons of the en group and the O/F atoms of the OTf^- anions, with distances ranging from 1.95 to 2.74 Å (Figure S11). Because of these hydrogen bonds, the cations of the heterometallic macrocycle **10a** form a one-dimensional rectangular channel, propagated along the *z* axis of the crystal (Figure 5b). A disordered molecule of methanol was found hosted in the cavity of the macrocycle, consistent with the result of the DOSY NMR experiment (Figure S41) which shows two diffusion constants for methanol: one corresponding to the bulk solvent and one that codiffuses with the cage. The single crystal structure of **10b** (Figure S10) is almost the same as **10a**, except with iridium centers instead of rhodium centers.

With the cavity increase of the macrocycle, the heterometallic macrocycles are large enough to accommodate some guest molecules. Tetrathiafulvalene (TTF), a well-known π-electron donor,[20] can be encapsulated by the heterometallic macrocycle **10a**. Within host **10a**, the encapsulated TTF guest's ^1H NMR signals were observed as two doublet at 7.33, 7.03 ppm, downfield from that of free TTF (6.46 ppm, CD_3OD). The solid state structure of **11** was determined by crystallographic analysis. As shown in Figure 5c,d, a TTF molecule is inserted in a centrosymmetric fashion through the center of the macrocycle **10a**, with a distance between the plane of the TTF unit and the plane of *L* of 3.4 Å.

CONCLUSIONS

In summary, a series of different type of multinuclear organometallic assemblies were constructed through stepwise coordination-driven self-assembly, by using a multifunctional hydroxamate ligand (*L*) featuring two pair of chelating sites together with half-sandwich iridium and rhodium fragments. It shows that the differences in the electron-donating ability of the two kinds of chelating sites played an important role in the formation of these assemblies. Remarkably, the tetranuclear half-sandwich iridium-based building block can be structurally regulated through the selective introduction of chloride ions to the *N*,*N*′-bonded iridium centers, resulting in the formation of "open" structures. Such an interesting selectivity is rare for most homometallic systems in which all metal ions have the same coordination environment. Furthermore, by making use of the different chemical hardness of the two types of metal-binding sites, heterometallic macrocycles **10a** and **10b** were constructed. These heterometallic macrocycles are large enough to be efficient hosts for the recognition of π-donor guests. Taken together, the findings in this study show that the ligand (*L*) provides a versatile scaffold for construct organometallic assemblies due to the discrimination between soft and hard binding sites. We hope that our results will help motivate the design of more effective new building blocks and the creation of increasingly complex systems, and advance the field of supramolecular assembly chemistry

EXPERIMENTAL SECTION

General Methods. All reagents and solvents were purchased from commercial sources and used as supplied unless otherwise mentioned. The starting materials $[Cp^*MCl_2]_2$ (M = Ir, Rh)[21] and 2,5-pyrazine-dicarboxylic acid dimethyl ester[22] were prepared by literature method. NMR spectra were recorded on Bruker AVANCE I 400 and VANCE-DMX 500 Spectrometers. Spectra were recorded at room temperature and referenced to the residual protonated solvent for NMR spectra. Coupling constants are expressed in hertz. Complex multiplets are noted as "m" and broad resonances as "br". Elemental analyses were performed on an Elementar Vario EL III analyzer. IR spectra of the solid samples (KBr tablets) in the range 400−4000 cm^{-1} were

DOI: 10.1021/jacs.5b08826
J. Am. Chem. Soc. 2015, 137, 13670−13678

recorded on a Nicolet AVATAR-360IR spectrometer. ESI-MS spectra were recorded on a Micro TOF II mass spectrometer using electrospray ionization.

Synthesis of Dipotassium Salt of Pyrazine-2,5-dihydroxamic Acid (H_2LK_2). Following a modified literature method,[23] hydroxylamine hydrochloride (781 mg, 11.2 mmol) was added to potassium hydroxide (1.259 g, 22.5 mmol) in methanol (12 mL). Precipitation of KCl was removed by filtration. The solution was then added dropwise to dimethyl pyrazine-2,5-dicarboxylate (551 mg, 2.8 mmol) in methanol (10 mL) in an ice bath. The mixture was then stirred for 24 h. A yellow, gelatinous precipitation was collected, washed with methanol (2 × 10 mL) and diethyl ether (2 × 10 mL) and dried in a vacuum.

H_2LK_2. 478 mg, yield: 62%. ^{1}H NMR (400 MHz, D_2O, ppm) δ = 8.89 (s, *L*-H). $^{13}C\{^1H\}$ NMR (101 MHz, D_2O, ppm) δ = 160.17, 147.53, 143.64, 141.34, 141.18. IR (KBr disk, cm^{-1}) ν = 3246, 1652, 1587, 1563, 1490, 1472, 1395, 1345, 1301, 1203, 1180, 1032, 896, 745, 672, 639, 527. Anal. Calcd for $C_6H_4K_2N_4O_4$: C, 26.27; H, 1.47; N, 20.42. Found: C, 26.30; H, 1.43; N, 20.51.

Synthesis of 1a,b. AgOTf (103 mg, 0.4 mmol) was added to a solution of $[Cp^*MCl_2]_2$ (0.1 mmol, M = Ir (80 mg), Rh (62 mg)) in CH_3OH (20 mL) at room temperature. The reaction mixture was stirred in the dark for 24 h and then filtered. H_2LK_2 (14 mg, 0.05 mmol) and *N*,*N*′-dimethylformamide (DMF) (0.5 mL) was added to the filtrate. The mixture was stirred at room temperature for 24 h to give a dark green solution. The solvent was concentrated to about 3 mL. Upon the addition of diethyl ether, a dark green solid was precipitated and collected, and dissolved by CH_2Cl_2. The dark red solution was filtered through a pad of Celite, and the product was recrystallized from a CH_2Cl_2/diethyl ether mixture to afford a black solid.

1a. 73 mg, yield: 68%. ^{1}H NMR (400 MHz, CD_3OD, ppm) δ = 8.99 (s, 2H, *L*-H), 1.83 (s, 30H, Cp*-H), 1.81 (s, 30H, Cp*-H). $^{13}C\{^1H\}$ NMR (101 MHz, CD_3OD, ppm) δ = 9.12 (Cp*), 9.63 (Cp*), 86.13 (Cp*), 92.21 (Cp*), 121.69 (q, J_{CF} = 320.0 Hz, SO_3CF_3), 145.40, 147.16, 171.72 (C═O). ^{19}F NMR (376 MHz, CD_3OD, ppm) δ = −80.0 (s, OTf^-). IR (KBr disk, cm^{-1}) ν = 2969, 2925, 1631, 1554, 1498, 1428, 1386, 1259, 1224, 1162, 1032, 952, 822, 757, 639, 554, 518. Anal. Calcd for $C_{50}H_{62}F_{12}Ir_4N_4O_{16}S_4{\cdot}2H_2O$: C, 28.11; H, 3.11; N, 2.62. Found: C, 28.04; H, 3.15; N, 2.57. ESI-MS *m*/*z* = 1953.1835 (calcd for $[M - 2H_2O, OTf]^+$ 1953.1843).

1b. 70 mg, yield: 79%. ^{1}H NMR (400 MHz, CD_3OD, ppm) δ = 8.93 (s, 2H, *L*-H), 1.81 (s, 30H, Cp*-H), 1.79 (s, 30H, Cp*-H). $^{13}C\{^1H\}$ NMR (101 MHz, CD_3OD, ppm) δ = 9.05 (Cp*), 9.06 (Cp*), 93.98 (Cp*), 99.49 (Cp*), 121.70 (q, J_{CF} = 320.8 Hz, SO_3CF_3), 143.90, 146.96, 165.13 (C═O). ^{19}F NMR (376 MHz, CD_3OD, ppm) δ = −80.0 (s, OTf^-). IR (KBr disk, cm^{-1}) ν = 2975, 2916, 1640, 1537, 1478, 1383, 1262, 1168, 1035, 946, 639, 583, 524. Anal. Calcd for $C_{50}H_{62}F_{12}Rh_4\ N_4O_{16}S_4{\cdot}2H_2O$: C, 33.76; H, 3.74; N, 3.15. Found: C, 33.83; H, 3.68; N, 3.09. ESI-MS *m*/*z* = 722.0005 (calcd for $[M - 2H_2O, OTf]^{2+}$ 722.0010), 1592.9538 (calcd for $[M - 2H_2O, OTf]^+$ 1592.9546).

General Synthesis of Octanuclear Cages. Pyrazine (6.4 mg, 0.08 mmol)/4,4′-bipyridine (bpy) (12.5 mg, 0.08 mmol)/*trans*-1,2-bis(4-pyridyl)-ethylene (bpe) (14.6 mg, 0.08 mmol) was added to a solution of **1a**/**1b** (0.04 mmol) in methanol. The mixture was then stirred for 24 h. The solution was filtered through Celite and evaporated to dryness. The product was crystallized from CH_3OH/ether.

2a. 79 mg, yield: 87%. ^{1}H NMR (400 MHz, CD_3OD, ppm) δ = 9.46−9.08(m), 8.96(s), 8.94(s), 8.90(s), 8.83(s), 8.78(s), 8.77(s), 8.74(s), 8.73(s), 8.51(m), 8.17(s), 7.90(s), 1.76−1.68 (m, Cp*-H). ^{19}F NMR (376 MHz, CD_3OD, ppm) δ = −79.6 (s, OTf^-). IR (KBr disk, cm^{-1}) ν = 3108, 2969, 2925, 1634, 1554, 1496, 1428, 1386, 1265, 1227, 1159, 1032, 952, 639, 554, 521. Anal. Calcd for $C_{116}H_{140}F_{24}Ir_8N_{16}O_{32}S_8$: C, 30.82; H, 3.12; N, 4.96. Found: C, 30.87; H, 3.14; N, 4.89.

2b. 60 mg, yield: 79%. ^{1}H NMR (400 MHz, CD_3OD, ppm) δ = 9.41−9.04(m), 9.02(s), 8.90(s), 8.85(s), 8.76(s), 8.71(s), 8.64(s), 8.47−8.28(m), 8.10(m), 7.71(m), 1.81−1.68 (m, Cp*-H). ^{19}F NMR (376 MHz, CD_3OD, ppm) δ = −79.6 (s, OTf^-). IR (KBr disk, cm^{-1}) ν = 3106, 2970, 2924, 1639, 1550, 1492, 1431, 1385, 1264, 1226, 1162, 1032, 952, 639, 560, 521. Anal. Calcd for $C_{116}H_{140}F_{24}Ir_8N_{16}O_{32}S_8$: C, 36.60; H, 3.71; N, 5.89. Found: C, 36.56; H, 3.74; N, 5.81.

3a. 80 mg, yield: 83%. D_2: ^{1}H NMR (400 MHz, CD_3OD, ppm) δ = 9.09 (s, 4H, *L*-H), 8.86 (d, *J* = 6.8 Hz, 8H, bpy-H), 8.48 (d, *J* = 6.8 Hz, 8H, bpy-H), 8.05 (d, *J* = 6.8 Hz, 8H, bpy-H), 7.88 (d, *J* = 6.8 Hz, 8H, bpy-H), 1.77 (s, 60H, Cp*-H), 1.70 (s, 60H, Cp*-H). C_{2h}: ^{1}H NMR (400 MHz, CD_3OD, ppm) δ 9.02 (s, 4H, *L*-H), 8.95 (d, *J* = 6.8 Hz, 8H, bpy-H), 8.37 (d, *J* = 6.8 Hz, 8H, bpy-H), 8.24 (d, *J* = 6.0 Hz, 8H, bpy-H), 7.45 (d, *J* = 6.4 Hz, 8H, bpy-H), 1.75 (s, 60H, Cp*-H), 1.73 (s, 60H, Cp*-H). ^{19}F NMR (376 MHz, CD_3OD, ppm) δ = −77.8 (s, $[OTf^- \subset \mathbf{3a}\text{-}D_2]$), −79.6 (s, OTf^-). IR (KBr disk, cm^{-1}) ν = 3102, 2969, 2925, 1614, 1549, 1490, 1419, 1383, 1280, 1259, 1226, 1162, 1032, 952, 822, 757, 639, 577, 521. Anal. Calcd for $C_{140}H_{156}F_{24}Ir_8N_{16}O_{32}S_8$: C, 34.85; H, 3.26; N, 4.64. Found: C, 34.91; H, 3.19; N, 4.57.

3b. 70 mg, yield: 85%. D_2: ^{1}H NMR (400 MHz, CD_3OD, ppm) δ = 9.04 (s, 4H, *L*-H), 8.79 (d, *J* = 6.4 Hz, 8H, bpy-H), 8.31 (d, *J* = 6.4 Hz, 8H, bpy-H), 7.97 (d, *J* = 6.4 Hz, 8H, bpy-H), 7.80 (d, *J* = 6.4 Hz, 8H, bpy-H), 1.81 (s, 60H, Cp*-H), 1.72−1.68 (m, 60H, Cp*-H). C_{2h}: ^{1}H NMR (400 MHz, CD_3OD, ppm) δ = 8.96 (s, 4H, *L*-H), 8.94 (d, *J* = 6.0 Hz, 8H, bpy-H), 8.36 (d, *J* = 6.0 Hz, 8H, bpy-H), 8.11 (d, *J* = 6.0 Hz, 8H, bpy-H), 7.41 (d, *J* = 6.0 Hz, 8H, bpy-H), 1.79 (s, 60H, Cp*-H), 1.78−1.74 (m, 60H, Cp*-H). ^{19}F NMR (376 MHz, CD_3OD, ppm) δ = −78.4 (s, $[OTf^- \subset \mathbf{3b}\text{-}D_2]$), −79.7 (s, OTf^-). IR (KBr disk, cm^{-1}) ν = 3101, 2970, 2922, 1610, 1541, 1484, 1415, 1384, 1279, 1259, 1224, 1160, 1031, 945, 822, 757, 639, 574, 518. Anal. Calcd for $C_{140}H_{156}F_{24}Rh_8N_{16}O_{32}S_8$: C, 40.91; H, 3.83; N, 5.45. Found: C, 40.79; H, 3.88; N, 5.39.

4. 68 mg, yield: 81%. D_2: ^{1}H NMR (400 MHz, CD_3OD, ppm) δ = 9.07 (s, 4H, *L*-H), 8.68 (d, *J* = 6.4 Hz, 8H, bpe-H), 8.10 (d, *J* = 6.4 Hz, 8H, bpe-H), 7.81 (d, *J* = 6.4 Hz, 8H, bpe-H), 7.51 (d, *J* = 6.4 Hz, 8H, bpe-H), 7.37 (d, *J* = 16.8 Hz, 4H, bpe-H), 7.47 (d, *J* = 16.8 Hz, 4H, bpe-H), 1.80 (s, 60H, Cp*-H), 1.74 (s, 60H, Cp*-H). C_{2h}: ^{1}H NMR (400 MHz, CD_3OD, ppm) δ = 8.98 (s, 4H, *L*-H), 8.77 (d, *J* = 5.6 Hz, 8H, bpe-H), 8.01−7.98 (m, 8H, bpy-H), 7.78 (s, 4H, bpe-H), 7.25 (d, *J* = 6.4 Hz, 8H, bpe-H), 7.11 (s, 4H, bpe-H), 1.78 (s, 60H, Cp*-H), 1.78 (s, 60H, Cp*-H). ^{19}F NMR (376 MHz, CD_3OD, ppm) δ = −79.7 (s, OTf^-). IR (KBr disk, cm^{-1}) ν = 3099, 2966, 2922, 1610, 1540, 1484, 1428, 1383, 1277, 1259, 1227, 1162, 1032, 946, 843, 639, 574, 518. Anal. Calcd for $C_{148}H_{164}F_{24}Rh_8N_{16}O_{32}S_8$: C, 42.18; H, 3.92; N, 5.32. Found: C, 42.29; H, 3.90; N, 5.25.

Synthesis of 5. AgOTf (77 mg, 0.3 mmol) was added to a solution of $[Cp^*IrCl_2]_2$ (80 mg, 0.1 mmol) in CH_3OH (20 mL) at room temperature and stirred in the dark for 24 h, followed by filtration to remove AgCl. H_2LK_2 (14 mg, 0.05 mmol) and DMF (0.5 mL) were added to the filtrate. The mixture was then stirred at room temperature for 24 h. A dark green solution was formed. The solvent was concentrated to about 3 mL. Upon the addition of diethyl ether, a dark green solid was precipitated and collected, and dissolved by CH_2Cl_2. The dark red solution was filtered through a pad of Celite, and the product was recrystallized from a CH_2Cl_2/diethyl ether mixture to afford a dark red solid.

5. 70 mg, yield: 80%. ^{1}H NMR (400 MHz, CD_3OD, ppm) δ = 8.82 (s, 2H, *L*-H), 1.84 (s, 15H, Cp*-H), 1.82 (s, 30H, Cp*-H), 1.82 (s, 15H, Cp*-H). ^{1}H NMR (400 MHz, $CDCl_3$, ppm) δ = 8.85 (s, 2H, *L*-H), 1.95 (s, 30H, Cp*-H), 1.83 (s, 30H, Cp*-H). $^{13}C\{^1H\}$ NMR (101 MHz, $CDCl_3$, ppm) δ = 8.99 (Cp*), 10.43 (Cp*), 88.04 (Cp*), 90.98 (Cp*), 120.78 (q, SO_3CF_3, J_{CF} = 321.8 Hz), 143.78, 147.58, 170.45 (C═O). IR (KBr disk, cm^{-1}) ν = 2970, 2922, 1658, 1631, 1546, 1462, 1404, 1384, 1272, 1223, 1152, 1032, 966, 638, 599, 573, 517. Anal. Calcd for $C_{48}H_{62}Cl_2F_6Ir_4N_4O_{10}S_2$: C, 30.78; H, 3.34; N, 2.99. Found: C, 30.84; H, 3.27; N, 2.93. ESI-MS *m*/*z* = 788.1326 (calcd for $[M - 2OTf]^{2+}$ 788.1303), 1725.2146 (calcd for $[M - 2OTf]^+$ 1725.2131).

Synthesis of Octanuclear Macrocycles. A mixture of pyrazine (3.2 mg, 0.04 mmol) and **5** (0.04 mmol) in CH_2Cl_2 (10 mL) was stirred for 24 h to give dark green solution. The solvent was concentrated to about 3 mL. Upon the addition of diethyl ether, a dark

DOI: 10.1021/jacs.5b08826
J. Am. Chem. Soc. 2015, 137, 13670−13678

green solid was precipitated and collected, and dissolved by CH_3OH. The product was crystallized from CH_3OH/diethyl ether.

6. 66 mg, yield: 85%. ^{1}H NMR (400 MHz, CD_3OD, ppm) δ = 9.16(s, 4H, *L*-H), 9.00−8.97(m, 1H, pyrazine-H), 8.86−8.72(m, 4H, pyrazine-H), 8.66−8.54(m, 3H, pyrazine-H), 1.87−1.61 (m, 120H, Cp*-H). IR (KBr disk, cm^{-1}) ν = 3104, 2970, 2923, 1551, 1495, 1425, 1404, 1386, 1262, 1224, 1158, 1031, 952, 825, 756, 639, 599, 573, 554, 518. Anal. Calcd for $C_{104}H_{132}Cl_4F_{12}Ir_8N_{12}O_{20}S_4$: C, 31.98; H, 3.41; N, 4.30. Found: C, 31.88; H, 3.46; N, 4.26.

Synthesis of Dodecanuclear Cage 7. A mixture of tpt (2,4,6-tri(4-pyridyl)-1,3,5-triazine) (6.3 mg, 0.02 mmol) and **5** (0.03 mmol) in CH_2Cl_2 (10 mL) was stirred for 24 h to give dark green solution. The dark red solution was filtered through a pad of Celite, and the product was crystallized from CH_2Cl_2/Hexane.

7. 53 mg, yield: 85%. ^{1}H NMR (400 MHz, CD_3OD, ppm) δ = 8.93−8.54 (m, 30H, *L*-H and tpt-H), 1.88−1.64 (m, 180H, Cp*-H). IR (KBr disk, cm^{-1}) ν = 2921, 1630, 1544, 1519, 1485, 1402, 1374, 1264, 1224, 1154, 1058, 1031, 954, 850, 812, 671, 645, 554, 517. Anal. Calcd for $C_{180}H_{210}Cl_6F_{18}Ir_{12}N_{24}O_{30}S_6$: C, 34.63; H, 3.39; N, 5.38. Found: C, 34.52; H, 3.35; N, 5.44

Synthesis of Heterometallic Complexes. *Synthesis of* ***8***. AgOTf (51 mg, 0.2 mmol) was added to a solution of (en)$PdCl_2$ (24 mg, 0.1 mmol) in CH_3OH (20 mL) at room temperature and stirred in the dark for 24 h, followed by filtration to remove AgCl. H_2LK_2 (14 mg, 0.05 mmol) and DMF (0.5 mL) were added to the filtrate. The mixture was then stirred at room temperature for 6 h. A purple red solution was formed. The solvent was concentrated to about 3 mL. Upon the addition of diethyl ether, a purple red solid was precipitated and collected, and dried under vacuum.

8. 40 mg, yield: 97%. ^{1}H NMR (400 MHz, DMSO-d_6, ppm) δ = 9.34 (s, 2H, −OH), 8.63 (s, 2H, *L*-H), 5.65 (br, 4H, −NH_2), 5.59 (br, 4H, −NH_2), 2.67 (br, 4H, −CH_2−), 2.60 (br, 4H, −CH_2−). IR (KBr disk, cm^{-1}) ν = 3246, 3154, 1633, 1485, 1383, 1258, 1229, 1168, 1032, 920, 761, 719, 640, 576, 519. Anal. Calcd for $C_{12}H_{20}F_6N_8O_{10}Pd_2S_2$: C, 17.42; H, 2.44; N, 13.54. Found: C, 17.36; H, 2.51; N, 13.60.

Synthesis of ***9a,b***. AgOTf (51 mg, 0.2 mmol) was added to a solution of $[Cp^*MCl_2]_2$ (0.05 mmol, M = Ir (40 mg), Rh (31 mg)) in CH_3OH (20 mL) at room temperature. The reaction mixture was stirred in the dark for 24 h and then filtered. DMF (0.5 mL) and **8** (0.05 mmol) was added to the filtrate. The reaction mixture was turned to a dark green solution in several minutes and stirred for 24 h. The solvent was concentrated to about 3 mL. Upon the addition of diethyl ether, a dark solid was precipitated and collected, and dried under vacuum. The product was crystallized from CH_3OH/DMF/diethyl ether.

9a. 70 mg, yield: 80%. ^{1}H NMR (400 MHz, CD_3OD, ppm) δ = 8.56 (s, 2H, *L*-H), 2.92−2.89 (m, 4H, −CH_2−), 2.86−2.83 (m, 4H, −CH_2−), 1.75 (s, 30H, Cp*-H). IR (KBr disk, cm^{-1}) ν = 3243, 3130, 1613, 1552, 1497, 1385, 1252, 1225, 1165, 1074, 1058, 1029, 955, 904, 758, 639, 575, 518. Anal. Calcd for $C_{34}H_{48}F_{12}Ir_2N_8O_{16}Pd_2S_4$: C, 22.96; H, 2.72; N, 6.30. Found: C, 22.87; H, 2.61; N, 6.22. ESI-MS *m*/*z* = 740.0056 (calcd for $[M - 2OTf]^{2+}$ 740.0076), 1628.9675 (calcd for $[M - OTf]^+$ 1628.9678).

9b. 66 mg, yield: 82%. ^{1}H NMR (400 MHz, CD_3OD, ppm) δ = 8.37 (s, 2H, *L*-H), 2.91−2.88 (m, 4H, −CH_2−), 2.85−2.82 (m, 4H, −CH_2−), 1.71 (s, 30H, Cp*-H). IR (KBr disk, cm^{-1}) ν = 3251, 1630, 1543, 1482, 1384, 1258, 1227, 1168, 1081, 1059, 1031, 952, 904, 759, 640, 576, 519. Anal. Calcd for $C_{34}H_{48}F_{12}Rh_2N_8O_{16}Pd_2S_4$: C, 25.53; H, 3.02; N, 7.00. Found: C, 25.46; H, 2.95; N, 7.08. ESI-MS *m*/*z* = 650.9572 (calcd for $[M + 2H - 2OTf]^{2+}$ 650.9588), 1450.8674 (calcd for $[M + 2H - OTf]^+$ 1450.8702).

Synthesis of ***10a,b***. A mixture of pyrazine (3.2 mg, 0.04 mmol) and **9a**/**9b** (0.04 mmol) in CH_3OH (20 mL) was stirred for 24 h to give dark green solution. The product was crystallized from CH_3OH/DMF/diethyl ether.

10a. 67 mg, yield: 90%. ^{1}H NMR (400 MHz, CD_3OD, ppm) δ = 8.84 (s, 8H, pyrazine-H), 8.36 (s, 4H, *L*-H), 5.98 (br, 4H, −NH_2), 5.78 (br, 4H, −NH_2), 5.47 (br, 4H, −NH_2), 4.98 (br, 4H, −NH_2), 3.00−2.77(m, 16H, −CH_2−), 1.61 (s, 60H, Cp*-H). IR (KBr disk, cm^{-1}) ν = 3251, 3158, 1660, 1606, 1552, 1498, 1423, 1386, 1254, 1166, 1109, 1079, 1031, 957, 760, 639, 576, 552, 519. Anal. Calcd for $C_{76}H_{104}F_{24}Ir_4N_{20}O_{32}Pd_4S_8$: C, 24.56; H, 2.82; N, 7.54. Found: C, 24.68; H, 2.77; N, 7.42.

10b. 61 mg, yield: 91%. ^{1}H NMR (400 MHz, CD_3OD, ppm) δ = 8.89 (s, 8H, pyrazine-H), 8.21 (s, 4H, *L*-H), 2.93−2.76 (m, 16H, −CH_2−), 1.65 (s, 60H, Cp*-H). IR (KBr disk, cm^{-1}) ν = 3243, 3143, 1629, 1545, 1487, 1420, 1384, 1256, 1226, 1163, 1081, 1060, 1030, 953, 758, 639, 575, 519, 493. Anal. Calcd for $C_{76}H_{104}F_{24}Rh_4N_{20}O_{32}Pd_4S_8$: C, 27.17; H, 3.12; N, 8.34. Found: C, 27.25; H, 3.16; N, 8.39.

Synthesis of ***11***. A mixture of tetrathiafulvalene (TTF) (1 mg, 0.005 mmol) and **10a** (19 mg, 0.005 mmol) in CH_3OH (20 mL) was stirred for 24 h. The product was crystallized from CH_3OH/diethyl ether.

11. 18 mg, yield: 93%. ^{1}H NMR (400 MHz, CD_3OD, ppm) δ = 9.03 (s, 8H, pyrazine-H), 8.34 (s, 4H, *L*-H), 5.94 (br, 4H, −NH_2), 5.66 (br, 4H, −NH_2), 5.30 (br, 4H, −NH_2), 4.78 (br, 4H, −NH_2), 2.92−2.81(m, 16H, −CH_2−), 1.63 (s, 60H, Cp*-H). Anal. Calcd for $C_{82}H_{108}F_{24}Ir_4N_{20}O_{32}Pd_4S_{12}$: C, 25.12; H, 2.78; N, 7.14. Found: C, 25.21; H, 2.69; N, 7.13.

■ ASSOCIATED CONTENT

Supporting Information

The Supporting Information is available free of charge on the ACS Publications website at DOI: 10.1021/jacs.5b08826.

Computational details, NMR spectra and crystallographic data. (PDF)

CIF files for complexes **1a**·2H_2O, **1a**·4CH_3CN, **1b**·4CH_3OH and **2b**-C_{2h}. (CIF)

CIF files for complexes $OTf^- \subset$ **3a**-D_2, **3b**-C_{2h}, **3b**-D_2 and $OTf^- \subset$ **3b**-D_2. (CIF)

CIF files for complexes **4**-D_2, **5**, **6**, **7**. (CIF)

CIF files for complexes **9b**, **10a**, **10b** and **11**. (CIF)

CIF files. (CIF)

CIF files. (CIF)

■ AUTHOR INFORMATION

Corresponding Author

*gxjin@fudan.edu.cn

Notes

The authors declare no competing financial interest.

■ ACKNOWLEDGMENTS

This work was supported by the National Science Foundation of China (21531002, 21374019), the National Basic Research Program of China (2015CB856600), the Shanghai Science and Technology Committee (13JC1400600) and the Program for Changjiang Scholars and Innovative Research Team in University (IRT1117).

■ REFERENCES

(1) (a) Gianneschi, N. C.; Masar, M. S.; Mirkin, C. A. *Acc. Chem. Res.* **2005**, *38*, 825−837. (b) Fujita, M.; Tominaga, M.; Hori, A.; Therrien, B. *Acc. Chem. Res.* **2005**, *38*, 369−378. (c) Pluth, M. D.; Bergman, R. G.; Raymond, K. N. *Acc. Chem. Res.* **2009**, *42*, 1650−1659. (d) Oliveri, C. G.; Ulmann, P. A.; Wiester, M. J.; Mirkin, C. A. *Acc. Chem. Res.* **2008**, *41*, 1618−1629. (e) Northrop, B. H.; Zheng, Y.-R.; Chi, K.-W.; Stang, P. J. *Acc. Chem. Res.* **2009**, *42*, 1554−1563. (f) De, S.; Mahata, K.; Schmittel, M. *Chem. Soc. Rev.* **2010**, *39*, 1555−1575.

(2) (a) Ariga, K.; Ito, H.; Hill, J. P.; Tsukube, H. *Chem. Soc. Rev.* **2012**, *41*, 5800−5835. (b) Chakrabarty, R.; Mukherjee, P. S.; Stang, P. J. *Chem. Rev.* **2011**, *111*, 6810−6918. (c) Amouri, H.; Desmarets, C.; Moussa, J. *Chem. Rev.* **2012**, *112*, 2015−2041. (d) Cook, T. R.; Zheng, Y. R.; Stang, P. J. *Chem. Rev.* **2013**, *113*, 734−777. (e) Smulders, M. M.; Riddell, I. A.; Browne, C.; Nitschke, J. R. *Chem. Soc. Rev.* **2013**, *42*,

DOI: 10.1021/jacs.5b08826
J. Am. Chem. Soc. 2015, 137, 13670−13678

1728−1754. (f) Cook, T. R.; Vajpayee, V.; Lee, M. H.; Stang, P. J.; Chi, K.-W. *Acc. Chem. Res.* **2013**, *46*, 2464−2474.
(3) (a) Ward, M. D.; Raithby, P. R. *Chem. Soc. Rev.* **2013**, *42*, 1619−1636. (b) Custelcean, R. *Chem. Soc. Rev.* **2014**, *43*, 1813−1824. (c) Schmidt, A.; Kühn, A. C. E. *Coord. Chem. Rev.* **2014**, *275*, 19−36. (d) Cook, T. R.; Stang, P. J. *Chem. Rev.* **2015**, *115*, 7001−7045. (e) Zarra, S.; Wood, D. M.; Roberts, D. A.; Nitscke, J. R. *Chem. Soc. Rev.* **2015**, *44*, 419−432. (f) Xu, L.; Wang, Y.-X.; Chen, L.-J.; Yang, H.-B. *Chem. Soc. Rev.* **2015**, *44*, 2148−2167.
(4) (a) Leigh, D. A.; Pritchard, R. G.; Stephens, A. J. *Nat. Chem.* **2014**, *6*, 978−982. (b) Wood, C. S.; Ronson, T. K.; Belenguer, A. M.; Holstein, J. J.; Nitschke, J. R. *Nat. Chem.* **2015**, *7*, 354−358. (c) Riddell, I. A.; Smulders, M. M. J.; Clegg, J. K.; Hristova, Y. R.; Breiner, B.; Thoburn, J. D.; Nitschke, J. R. *Nat. Chem.* **2012**, *4*, 751−756. (d) Freye, S.; Hey, J.; Torras-Galán, A.; Stalke, D.; Herbst-Irmer, R.; John, M.; Clever, G. H. *Angew. Chem., Int. Ed.* **2012**, *51*, 2191−2194. (e) Zheng, Y.-R.; Lan, W.-J.; Wang, M.; Cook, T. R.; Stang, P. J. *J. Am. Chem. Soc.* **2011**, *133*, 17045−17055. (f) Mukherjee, S.; Mukherjee, P. S. *Chem. Commun.* **2014**, *50*, 2239−2248.
(5) (a) Wang, Z. J.; Clary, K. N.; Bergman, R. G.; Raymond, K. N.; Toste, F. D. *Nat. Chem.* **2013**, *5*, 100−103. (b) Wiester, M. J.; Ulmann, P. A.; Mirkin, C. A. *Angew. Chem., Int. Ed.* **2011**, *50*, 114−137. (c) Yoshizawa, M.; Klosterman, J. K.; Fujita, M. *Angew. Chem., Int. Ed.* **2009**, *48*, 3418−3438. (d) Inokuma, Y.; Kawano, M.; Fujita, M. *Nat. Chem.* **2011**, *3*, 349−358. (e) Grishagin, I. V.; Pollock, J. B.; Kushal, S.; Cook, T. R.; Stang, P. J.; Olenyuk, B. Z. *Proc. Natl. Acad. Sci. U. S. A.* **2014**, *111*, 18448−18453. (f) Yan, X.; Cook, T. R.; Wang, P.; Huang, F.; Stang, P. J. *Nat. Chem.* **2015**, *7*, 342−348. (g) Chen, L.-J.; Ren, Y.-Y.; Wu, N.-W.; Sun, B.; Ma, J.-Q.; Zhang, L.; Tan, H.; Liu, M.; Li, X.; Yang, H.-B. *J. Am. Chem. Soc.* **2015**, *137*, 11725−11735. (h) Kieltyka, R.; Englebienne, P.; Fakhoury, J.; Autexier, C.; Moitessier, N.; Sleiman, H. F. *J. Am. Chem. Soc.* **2008**, *130*, 10040−10041.
(6) (a) Steed, J. W.; Turner, D. R.; Wallace, K. J. *Core Concepts in Supramolecular Chemistry and Nanochemistry*; John Wiley & Sons: West Sussex, U.K., 2007. (b) Steed, J. W.; Atwood, J. L. *Supramolecular Chemistry*; John Wiley & Sons: West Sussex, U.K., 2000.
(7) (a) Saalfrank, R. W.; Löw, N.; Kareth, S.; Seitz, V.; Hampel, F.; Stalke, D.; Teichert, M. *Angew. Chem., Int. Ed.* **1998**, *37*, 172−175. (b) Schmittel, M.; Mahata, K. *Angew. Chem., Int. Ed.* **2008**, *47*, 5284−5286. (c) Meeuwissen, J.; Reek, J. N. H. *Nat. Chem.* **2011**, *2*, 615−621. (d) Park, J. S.; Lifschitz, A. M.; Young, R. M.; Mendez-Arroyo, J.; Wasielewski, M. R.; Stern, C. L.; Mirkin, C. A. *J. Am. Chem. Soc.* **2013**, *135*, 16988−16996. (e) Li, H.; Yao, Z.-J.; Liu, D.; Jin, G.-X. *Coord. Chem. Rev.* **2015**, *293*, 139−157. (f) Park, Y. J.; Ryu, J. Y.; Begum, H.; Lee, M. H.; Stang, P. J.; Lee, J. *J. Am. Chem. Soc.* **2015**, *137*, 5863−5866. (g) Bhat, I. A.; Samanta, D.; Mukherjee, P. S. *J. Am. Chem. Soc.* **2015**, *137*, 9497−9502.
(8) (a) Farrell, J. R.; Mirkin, C. A.; Guzei, I. A.; Liable-Sands, L. M.; Rheingold, A. L. *Angew. Chem., Int. Ed.* **1998**, *37*, 465−467. (b) Sun, X.; Johnson, D. W.; Caulder, D. L.; Powers, R. E.; Raymond, K. N.; Wong, E. H. *Angew. Chem., Int. Ed.* **1999**, *38*, 1303−1307. (c) Hahn, F. E.; Offermann, M.; Schulze Isfort, C.; Pape, T.; Fröhlich, R. *Angew. Chem., Int. Ed.* **2008**, *47*, 6794−6797. (d) Maity, R.; Koppetz, H.; Hepp, A.; Hahn, F. E. *J. Am. Chem. Soc.* **2013**, *135*, 4966−4969. (e) Sun, Q.-F.; Sato, S.; Fujita, M. *Nat. Chem.* **2012**, *4*, 330−333. (f) Bandi, S.; Pal, A. K.; Hanan, G. S.; Chand, D. K. *Chem. - Eur. J.* **2014**, *20*, 13122−13126. (g) Schouwey, C.; Holstein, J. J.; Scopelliti, R.; Zhurov, K. O.; Nagornov, K. O.; Tsybin, Y. O.; Smart, O. S.; Bricogne, G.; Severin, K. *Angew. Chem., Int. Ed.* **2014**, *53*, 11261−11265.
(9) (a) Chatterjee, B. *Coord. Chem. Rev.* **1978**, *26*, 281−303. (b) Miller, M. J. *Chem. Rev.* **1989**, *89*, 1563−1579. (c) Kurzak, B.; Kozlowski, H.; Farkas, E. *Coord. Chem. Rev.* **1992**, *114*, 169−200. (d) Marmion, C. J.; Murphy, T.; Docherty, J. R.; Nolan, K. B. *Chem. Commun.* **2000**, 1153−1154. (e) Codd, R. *Coord. Chem. Rev.* **2008**, *252*, 1387−1408. (f) Bodwin, J. J.; Cutland, A. D.; Malkani, R. G.; Pecoraro, V. L. *Coord. Chem. Rev.* **2001**, *216*, 489−512. (g) Mezei, G.; Zaleski, C. M.; Pecoraro, V. L. *Chem. Rev.* **2007**, *107*, 4933−5003.
(10) (a) Beissel, T.; Powers, R. E.; Parac, T. N.; Raymond, K. N. *J. Am. Chem. Soc.* **1999**, *121*, 4200−4206. (b) Bai, Y.; Guo, D.; Duan, C.-Y.; Dang, D.-B.; Pang, K.-L.; Meng, Q.-J. *Chem. Commun.* **2004**, 186−187.
(11) (a) Golenya, I. A.; Gumienna-Kontecka, E.; Boyko, A. N.; Haukka, M.; Fritsky, I. O. *Inorg. Chem.* **2012**, *51*, 6221−6227. (b) Jankolovits, J.; Kampf, J. W.; Pecoraro, V. L. *Inorg. Chem.* **2013**, *52*, 5063−5076.
(12) (a) Severin, K. *Chem. Commun.* **2006**, 3859−3867. (b) Boyer, J. L.; Kuhlman, M. L.; Rauchfuss, T. B. *Acc. Chem. Res.* **2007**, *40*, 233−242. (c) Conrady, F. M.; Fröhlich, R.; Schulte to Brinke, C.; Pape, T.; Hahn, F. E. *J. Am. Chem. Soc.* **2011**, *133*, 11496−11499. (d) Han, Y.-F.; Jin, G.-X. *Acc. Chem. Res.* **2014**, *47*, 3571−3579. (e) Singh, N.; Jo, J.-H.; Song, Y. H.; Kim, H.; Kim, D.; Lah, M. S.; Chi, K.-W. *Chem. Commun.* **2015**, *51*, 4492−4495. (f) Mirtschin, S.; Slabon-Turski, A.; Scopelliti, R.; Velders, A. H.; Severin, K. *J. Am. Chem. Soc.* **2010**, *132*, 14004. (g) Singh, A. K.; Pandey, D. S.; Xu, Q.; Braunstein, P. *Coord. Chem. Rev.* **2014**, *270*, 31−56. (h) Pitto-Barry, A.; Barry, N. P. E.; Russo, V.; Heinrich, B.; Donnio, B.; Therrien, B.; Deschenaux, R. *J. Am. Chem. Soc.* **2014**, *136*, 17616−17625.
(13) (a) Mirtschin, S.; Krasniqi, E.; Scopelliti, R.; Severin, K. *Inorg. Chem.* **2008**, *47*, 6375−6381. (b) Shanmugaraju, S.; Bar, A. K.; Mukherjee, P. S. *Inorg. Chem.* **2010**, *49*, 10235−10237. (c) Pitto-Barry, A.; Barry, N. P. E.; Zava, O.; Deschenaux, R.; Dyson, P. J.; Therrien, B. *Chem. - Eur. J.* **2011**, *17*, 1966−1971.
(14) (a) Huang, S.-L.; Lin, Y.-J.; Hor, T. S. A.; Jin, G.-X. *J. Am. Chem. Soc.* **2013**, *135*, 8125−8128. (b) Li, H.; Han, Y.-F.; Lin, Y.-J.; Guo, Z.-W.; Jin, G.-X. *J. Am. Chem. Soc.* **2014**, *136*, 2982−2985.
(15) (a) Lehaire, M.-L.; Scopelliti, R.; Piotrowski, H.; Severin, K. *Angew. Chem., Int. Ed.* **2002**, *41*, 1419−1422. (b) Grote, Z.; Scopelliti, R.; Severin, K. *J. Am. Chem. Soc.* **2004**, *126*, 16959−16972. (c) Vajpayee, V.; Song, Y. H.; Lee, M. H.; Kim, H.; Wang, M.; Stang, P. J.; Chi, K.-W. *Chem. - Eur. J.* **2011**, *17*, 7837−7844. (d) Wang, M.; Vajpayee, V.; Shanmugaraju, S.; Zheng, Y.-R.; Zhao, Z.; Kim, H.; Mukherjee, P. S.; Chi, K.-W.; Stang, P. J. *Inorg. Chem.* **2011**, *50*, 1506−1512.
(16) (a) Therrien, B.; Süss-Fink, G.; Govindaswamy, P.; Renfrew, A. K.; Dyson, P. J. *Angew. Chem., Int. Ed.* **2008**, *47*, 3773−3776. (b) Zava, O.; Mattsson, J.; Therrien, B.; Dyson, P. J. *Chem. - Eur. J.* **2010**, *16*, 1428−1431. (c) Barry, N. P. E.; Zava, O.; Dyson, P. J.; Therrien, B. *Chem. - Eur. J.* **2011**, *17*, 9669−9677. (d) Schmitt, F.; Freud-enreich, J.; Barry, N. P. E.; Juillerat-Jeanneret, L.; Süss-Fink, G.; Therrien, B. *J. Am. Chem. Soc.* **2012**, *134*, 754−757.
(17) (a) Espinet, P.; Bailey, P. M.; Maitlis, P. M. *J. Chem. Soc., Dalton Trans.* **1979**, 1542−1547. (b) Blacker, A. J.; Clot, E.; Duckett, S. B.; Eisenstein, O.; Grace, J.; Nova, A.; Perutz, R. N.; Taylor, D. J.; Whitwood, A. C. *Chem. Commun.* **2009**, 6801−6803. (c) Zamorano, A.; Rendón, N.; López-Serrano, J.; Valpuesta, J. E. V.; Álvarez, E.; Carmona, E. *Chem. - Eur. J.* **2015**, *21*, 2576−2587.
(18) (a) Lunder, D. M.; Lobkovsky, E. B.; Streib, W. E.; Caulton, K. G. *J. Am. Chem. Soc.* **1991**, *113*, 1837−1838. (b) Flood, T. C.; Lim, J. K.; Deming, M. A.; Keung, W. *Organometallics* **2000**, *19*, 1166−1174. (c) Bhalla, G.; Liu, X. Y.; Oxgaard, J.; Goddard, W. A., III; Periana, R. A. *J. Am. Chem. Soc.* **2005**, *127*, 11372−11389.
(19) (a) Griffith, D. M.; Bíró, L.; Platts, J. A.; Müller-Bunz, H.; Farkas, E.; Buglyó, P. *Inorg. Chim. Acta* **2012**, *380*, 291−300. (b) Griffith, D.; Lyssenko, K.; Jensen, P.; Kruger, P. E.; Marmion, C. J. *Dalton Trans.* **2005**, 956−961. (c) Hall, M. D.; Failes, T. W.; Hibbs, D. E.; Hambley, T. W. *Inorg. Chem.* **2002**, *41*, 1223−1228.
(20) (a) Philp, D.; Slawin, A. M. Z.; Spencer, N.; Stoddart, J. F.; Williams, D. J. *J. Chem. Soc., Chem. Commun.* **1991**, 1584−1586. (b) Jørgensen, T.; Hansen, T. K.; Becher, J. *Chem. Soc. Rev.* **1994**, *23*, 41−51. (c) Yoshizawa, M.; Kumazawa, K.; Fujita, M. *J. Am. Chem. Soc.* **2015**, *127*, 13456−13457.
(21) White, C.; Yates, A.; Maitlis, P. M. *Inorg. Synth.* **1992**, *29*, 228−234.
(22) Cockriel, D. L.; McClain, J. M.; Patel, K. C.; Ullom, R.; Hasley, T. R.; Archibald, S. J.; Hubin, T. J. *Inorg. Chem. Commun.* **2008**, *11*, 1−4.

DOI: 10.1021/jacs.5b08826
J. Am. Chem. Soc. 2015, 137, 13670−13678

(23) Griffith, D.; Chopra, A.; Müller-Bunz, H.; Marmion, C. J. *Dalton Trans.* **2008**, 6933−6939.

DOI: 10.1021/jacs.5b08826
J. Am. Chem. Soc. 2015, 137, 13670−13678